Characterizing Coverage and Downlink Throughput of Cloud Empowered HetNets

Syed Ali Raza Zaidi, *Member, IEEE*, Ali Imran, *Member, IEEE*,
Desmond C. McLernon, *Member, IEEE*, and Mounir Ghogho, *Senior Member, IEEE*

***Abstract*—In this letter, we introduce the concept of cloud empowered heterogeneous networks. We propose a simple yet efficient association mechanism for the selection of a serving remote radio head (RRH) for a desired mobile user (MU). We introduce the concept of user centric clustering which improves the user throughput by contributing on several fronts. Employing well established tools from stochastic geometry, we characterize the downlink coverage probability for the MU. The coverage probability is in turn employed to characterize the attainable throughput at a certain desired reliability constraint. Simulation results are presented to indicate the gains experienced by employing additional tiers in a cloud radio access network(C-RAN). Such gains are attributed to the distributed diversity which provides a power gain and hence increases the effective received SNR.**

***Index Terms*—Cloud radio access networks, heterogeneous network, coverage, throughput, Poisson process.**

I. Introduction

CLOUD radio access networks (C-RANs) are envisioned to provide a new path-way towards the deployment of small cellular networks [1]. A C-RAN architecture decouples the baseband processing unit (BBU) from the remote radio head (RRH). RRHs are connected to the cloud BBU pool via a flexible front-haul which is usually a fiber optic cable. It has been shown that such a flexible architecture: (i) reduces the capital and operational expenditure; (ii) provides huge energy saving (due to centralized air-conditioning, etc.) and (iii) provisions implementation of sophisticated coordination mechanisms for reducing the co-channel interference (e.g., like using coordinated multipoint (CoMP) transmission, interference alignment etc.) [2]. Because of the centralized processing, the interference management techniques in a C-RAN are virtually overhead-free [2] when compared to the traditional small cellular network where control, coordination and synchronization overheads are significant.

The above-mentioned advantages of a C-RAN have recently triggered significant interest in both industry [1], [3], [4] and academia [2], [6]–[8] to investigate the design space of C-RAN based small cellular networks. Since most of these developments are very recent much of the design space remains an uncharted territory.

In this article, we take a step further and propose the C-RAN enabled small cellular heterogeneous network (HetNet). The heterogeneity in terms of cell types and RRHs will allow the operator to further increase the data rate. The added benefit of C-RAN is that due to centralized processing the co-channel interference can be effectively eliminated. To the best of our knowledge, cloud HetNets have not been explored in the past. Hence in this article, we take a first step towards characterizing the coverage and the attainable downlink throughput for an arbitrary MU in a heterogeneous C-RAN. We model the heterogeneous C-RAN as a K-tier network with different RRH densities and transmit powers employed at each tier.

II. Contributions and Organization

The contribution of this article is twofold:

1) First, we introduce a user centric RRH clustering mechanism and propose a simple association mechanism for the MU in a K-tier C-RAN (see Section IV). We then characterize the coverage probability of an arbitrary MU at a desired signal-to-noise ratio (SNR) threshold. Our analysis accounts for both the channel and the spatial variations (see Section III) present in the downlink of a C-RAN.
2) Second, the developed analytical framework is utilized to derive an upper-bound on the attainable bits/s/Hz performance of a $K-$tier network under a certain reliability constraint (see Section V). The reliability constraint and the SNR threshold can be considered as a proxy for the MU's desired quality of service (QoS). Lastly, we investigate the attainable throughput gains which can be realized by deploying additional tiers with the decreasing transmit power.

A. Notation

Throughout the paper, a particular realization of a random variable Z is denoted by a corresponding lower-case letter z and its corresponding probability density function (PDF) is denoted by $f_Z(.)$. The boldface lower-case letter (e.g., $\boldsymbol{x}$) is employed to denote a vector in $\mathbb{R}^2$. For sake of compactness, we employ $\boldsymbol{x}$ to refer to the vector itself and its location as well. The symbol $\setminus$ denotes the set subtraction and $\|\boldsymbol{x}\|$ denotes the Euclidean norm of the vector $\boldsymbol{x}$. The symbol $b(\boldsymbol{x}, r)$ denotes a ball of radius r centered at point $\boldsymbol{x}$. The symbol $\in$ denotes set membership and Π is generally employed to denote the point process. The point process is also used as a counting measure by using the notation $\Pi(\mathcal{A})$ which returns the number of points in Π which lie inside $\mathcal{A} \in \mathbb{R}^2$. The symbol $Z \sim \mathcal{CN}(a, b)$ is used to denote a complex normal random variable with mean a and variance b. Finally, $Z \sim \mathcal{E}(\mu)$ is used to denote an exponential random variable with mean μ.

Manuscript received August 9, 2014; revised January 16, 2015; accepted January 19, 2015. Date of publication February 9, 2015; date of current version June 5, 2015. This work was made possible by NPRP grant No. 5-1047-2-437 from the Qatar National Research Fund (a member of The Qatar Foundation). The statements made herein are solely the responsibility of the authors. The associate editor coordinating the review of this paper and approving it for publication was J. Lee.

S. A. R. Zaidi and D. C. McLernon are with the School of Electronics and Electrical Engineering, University of Leeds, Leeds LS2 9JT, U.K. (e-mail: elsarz@leeds.ac.uk; d.c.mclernon@leeds.ac.uk).

A. Imran is with School of Electrical and Computer Engineering, Oklahoma University, Norman, OK 73019-1102 USA (e-mail: ali.imran@ou.edu).

M. Ghogho is with the School of Electronics and Electrical Engineering, University of Leeds, Leeds LS2 9JT, U.K. He is also with Department of Electronics, Logistics, Informatics and Telecommunications, University International Rabat, 10000 Rabat, Morocco (e-mail: m.ghogho@leeds.ac.uk).

Digital Object Identifier 10.1109/LCOMM.2015.2401565

III. Network Model

A. Spatial Model for HetNet RRHs

We consider a K-tier C-RAN HetNet such that the first tier is formed by the macro cellular BS. The subsequent $K-1$ tiers correspond to small cellular RRHs, such as femto and pico cellular networks. We assume that all tiers are connected to a cloud data center which hosts the BBU pool. The spatial configuration of the RRHs in the kth tier is modeled using a homogeneous Poisson point process (HPPP), Π_k, with intensity λ_k for $k \in K$. Specifically, at an arbitrary time instant the probability of finding $n_k \in \mathbb{N}$ RRHs inside a typical area foot-print $\mathcal{A} \subseteq \mathbb{R}^2$ follows the Poisson law with mean measure $\Lambda_k(\mathcal{A}) = \lambda_k v_2(\mathcal{A})$. The mean measure is characterized by both the average number of kth-tier RRHs per unit area (i.e., λ_k) and the Lebesgue measure [8] $v_2(\mathcal{A}) = \int_{\mathcal{A}} d\boldsymbol{x}$ on $\mathbb{R}^2$, where if $\mathcal{A}$ is a disc of radius r then $v_2(\mathcal{A}) = \pi r^2$ is the area of the disc. Given $n_k \in \mathbb{N}$, the RRHs are uniformly distributed in $\mathcal{A} \subseteq \mathbb{R}^2$. Notice that effectively K-tier C-RAN HetNet is formed by K independent and identically distributed (i.i.d.) HPPPs, i.e., $\Pi = \cup_{k=1}^{K} \Pi_k$ which follows from the superposition theorem for HPPPs (see [8]).

B. User Centric Clustering and Frequency Allocation

Without loss of generality, we focus on an arbitrary MU $\boldsymbol{u}$ located at the origin. We assume that the cloud data center performs user centric clustering, i.e., an arbitrary user is served by the HetNet RRHs which lie within a cluster of radius $\mathcal{R}_c$. Notice that such user centric clustering is beneficial on several fronts:

1) It allows the C-RAN data center to control the maximum number of activated RRHs and hence the total amount of energy spent on serving the user. It also allows sleep scheduling of both the RRH and BBUs, as they are only activated on a demand basis;
2) Limiting RRH selection within a disc of radius $\mathcal{R}_c$ also allows the C-RAN to control the worst case attenuation due to path-loss. Given a typical user's QoS requirement, C-RAN can employ a self-organization mechanism to dimension the cluster radius in an optimal manner;
3) In a saturated network, where multiple users are served in each macrocell at the same time, it allows aggressive frequency reuse by allowing inherent interference protection. C-RAN ensures that the clusters do not spatially overlap, hence introducing a guard zone for each user.

In this paper, we assume that the C-RAN partitions the available bandwidth into sub-channels. Each cluster is assigned one of these sub-channels. Furthermore, we assume that the sub-channel allocation can be done in an interference free manner.

C. Channel Model

The channel between a kth-tier C-RAN RRH $\boldsymbol{x_j} \in \Pi_k$ and the MU $\boldsymbol{u}$ is modeled by $H_{j,k} l_k(\|\boldsymbol{x_j}\|)$. Here $H_{j,k} \sim \mathcal{E}(1)$ is a unit mean exponential random variable which captures the impact of Rayleigh fading channel between an RRH and MU. The small-scale Rayleigh fading is complemented by a large-scale path-loss modeled by $l_k(\|\boldsymbol{x_j}\|) = G_k \max(r_o, \|\boldsymbol{x_j}\|)^{-\alpha_k}$. Here r_o is the reference distance; $\|\boldsymbol{x}_j\|$ is distance between the RRH and the MU; G_k is a frequency dependent constant and $\alpha_k \geq 2$ is an environment/terrain dependent path-loss exponent for for the kth-tier. The fading channel gains are assumed to be mutually independent and identically distributed (i.i.d.).

IV. Coverage Analysis for K-Tier C-RAN Downlink

A. RRH Selection and Signal Model

In this article, we consider a scenario where the MU is associated with the RRH which maximizes its received SNR. More specifically, we consider that as a first step, the MU shortlists the best RRH in each of the K-tiers. Out of these K-best RRHs, the one which will result in the best received SNR is scheduled to serve the user. The proposed association mechanism can be implemented as follows:

- **Step 1**: The macro BS which is closest to the user $\boldsymbol{u}$, transmits a pilot to the user $\boldsymbol{u}$.
- **Step 2**: The MU $\boldsymbol{u}$ simply retransmits the pilot signal.
- **Step 3**: Each RRH inside the user cluster $b(\boldsymbol{u}, \mathcal{R}_c)$ estimates the channel gain between the MU and itself. Here $\mathcal{R}_c$ denotes the cluster radius.
- **Step 4**: These channel gains are reported to the data center which schedules the data transmission on the BBU corresponding to the best RRH.

Under the proposed association scheme, the received signal at the MU $\boldsymbol{u}$ can be written as

$$s_{\boldsymbol{u}}^{\{rx\}} = \sqrt{\max_{i=1\ldots K} P_i \zeta_i \left(\underbrace{\Pi_i \cap b(\boldsymbol{u}, \mathcal{R}_c)}_{\mathcal{S}_i} \right)} s_{\boldsymbol{u}} + w_{\boldsymbol{u}} \tag{1}$$

where $\zeta_i(\mathcal{S}_i) = \max_{j \in \mathcal{S}_i} h_{j,i} l_i(r_j)$ is the channel gain between the serving RRH and the MU, $s_{\boldsymbol{u}} \sim \mathcal{CN}(0,1)$ is the transmitted data signal and $w_{\boldsymbol{u}} \sim \mathcal{CN}(0, \sigma^2)$ is the additive white Gaussian noise (AWGN) at the receiver front end. From (1) the received SNR can be computed as follows

$$\text{SNR} = \Gamma_{\boldsymbol{u}} = \frac{\max_{i=1\ldots K} P_i \zeta_i(\mathcal{S}_i)}{\sigma^2}. \tag{2}$$

B. Coverage Probability for the MU

Proposition 1: The CDF of the channel gain between the best RRH in the ith-tier and the MU, $\zeta_i(\mathcal{S}_i) = \max_{j \in \mathcal{S}_i} h_{j,i} l_i(r_j)$ is given by

$$\mathcal{F}_{\zeta_i}(z) = \exp\left[-\lambda_i \pi \left\{ r_o^2 \exp\left(-\frac{z r_o^{\alpha_i}}{G_i} \right) + \delta_i (G_i z^{-1})^{\delta_i} \times \left(\gamma_l\left(\delta_i, \frac{z \mathcal{R}_c^{\alpha_i}}{G_i} \right) - \gamma_l\left(\delta_i, \frac{z r_o^{\alpha_i}}{G_i} \right) \right) \right\} \right] \tag{3}$$

where $\gamma_l(a,b) = \int_o^b t^{a-1} \exp(-t) dt$ is the lower incomplete Gamma function and $\delta_i = 2/\alpha_i$ is the path-loss dependent constant.

Proof: Consider the marked Poisson point process [8] $\bar{\Pi}_i(z)$ which is constructed from the HPPP Π_i as follows

$$\bar{\Pi}_i(z) = \{ [\boldsymbol{y}, h_{y,i}, \mathbf{1}_z (h_{y,i} l_i(\|\boldsymbol{y}\|))] : \forall \boldsymbol{y} \in \Pi_i \}. \tag{4}$$

In other words, each point in Π_i is assigned a mark $h_{\boldsymbol{y},i} \sim \mathcal{E}(1)$ which captures the small-scale Rayleigh fading channel between the RRH and the MU. Notice that these marks are i.i.d. and do not depend on the location or the tier index. Furthermore, each point is assigned an additional indicator/Bernoulli mark $\mathbb{1}_z(h_{y,i} l_i(\|\boldsymbol{y}\|))$ which can be defined as

$$\mathbf{1}_z (h_{y,i} l_i (\|\boldsymbol{y}\|)) = \begin{cases} 1 & \text{if } h_{y,i} l_i (\|\boldsymbol{y}\|) \geq z \\ 0 & \text{otherwise.} \end{cases} \tag{5}$$

Notice that these indicator random variables are dependent upon both the fading and the distance between the MU and the RRH. Effectively, the marked Poisson process $\bar{\Pi}_i(z)$ represents all RRHs whose composite fading and path-loss propagation

gain exceeds certain desired value z. Consequently, the relationship between void probability of the $\bar{\Pi}_i(z)$ and CDF of $\zeta_i(\mathcal{S}_i)$ can be established as follows

$$\begin{aligned}\mathcal{F}_{\zeta_i}(z) &= \Pr\{\zeta_i \le z\} = \Pr\left\{\bar{\Pi}_i(z) = \emptyset\right\}, \\ &= \exp\left(-\Lambda_i\left(b(o,\mathcal{R}_c), z\right)\right) \end{aligned} \tag{6}$$

where $\Lambda_i(\mathcal{A}, z)$ is the mean measure of the $\bar{\Pi}_i(z)$ over an area $\mathcal{A} \in \mathbb{R}^2$. Employing the theory of a marked Poisson point process from [8], the mean measure $\Lambda_i(b(o,\mathcal{R}_c), z)$ can be computed as follows

$$\begin{aligned}&\Lambda_i\left(b(o,\mathcal{R}_c), z\right) \\ &= \int_0^{\infty}\int_{b(o,\mathcal{R}_c)} \lambda_i(\boldsymbol{x}, h)d\boldsymbol{x}dh = \int_0^{\infty}\int_0^{\mathcal{R}_c} 2\pi\lambda_i r \mathbf{1}_z(hl_i(r))f_H(h)dhdr, \\ &= \lambda_i\left[\pi r_o^2 \exp\left(-\frac{z}{G_i}r_o^{\alpha}\right)dr + \underbrace{\int_{r_o}^{\mathcal{R}_c} 2\pi r \exp\left(-\frac{z}{G_i}r^{\alpha_i}\right)dr}_{B_1}\right] \end{aligned} \tag{7}$$

The integral in B_1 can be evaluated by substituting $u = (z/G_i)r^{\alpha_i}$ as follows

$$\begin{aligned}B_1 &= \pi\int_{r_o}^{\mathcal{R}_c} 2r\exp\left(-\frac{z}{G_i}r^{\alpha_i}\right)dr = \delta_i\pi\frac{G_i^{\delta_i}}{z^{\delta_i}}\int_{\frac{z}{G_i}r_o^{\alpha_i}}^{\frac{z}{G_i}\mathcal{R}_c^{\alpha_i}} u^{\delta_i-1}\exp(u)du, \\ &\overset{(a)}{=} \delta_i\pi\frac{G_i^{\delta_i}}{z^{\delta_i}}\left[\gamma_l\left(\delta_i, \frac{z\mathcal{R}_c^{\alpha_i}}{G_i}\right) - \gamma_l\left(\delta_i, \frac{zr_o^{\alpha_i}}{G_i}\right)\right] \end{aligned} \tag{8}$$

where (a) follows from the definition of lower incomplete Gamma function i.e., $\gamma_l(a,b) = \int_o^b t^{a-1}\exp(-t)dt$; and $\delta_i = 2/\alpha_i$ is a path-loss dependent constant. Substituting B_1 into (7) and then employing (6) concludes the proof. ■

Proposition 2: The probability that the MU can be covered by the scheduled RRH at a certain desired SNR threshold γ_{th} under the proposed RRH selection scheme can be quantified as

$$\begin{aligned}\mathbb{P}_{cov} = \Pr\{\Gamma_u \ge \gamma_{th}\} = 1 - \prod_{i=1}^{K}\exp\Bigg[-\lambda_i\pi\Bigg\{r_o^2\exp\left(-\frac{\tilde{\gamma}_{th}r_o^{\alpha_i}}{\tilde{P}_i}\right) \\ + \delta_i\tilde{P}_i^{\delta_i}\tilde{\gamma}_{th}^{-\delta_i}\left(\gamma_l\left(\delta_i, \frac{\tilde{\gamma}_{th}\mathcal{R}_c^{\alpha_i}}{\tilde{P}_i}\right) - \gamma_l\left(\delta_i, \frac{\tilde{\gamma}_{th}r_o^{\alpha_i}}{\tilde{P}_i}\right)\right)\Bigg\}\Bigg], \end{aligned} \tag{9}$$

where $\tilde{\gamma}_{th} = \gamma_{th}\sigma^2$ can be considered as the normalized SNR threshold with respect to the received SNR in the absence of fading and path-loss when unit transmit power is employed, $\tilde{P}_i = P_iG_i$ is the total received power considering the frequency and antenna dependent gain G_i and $\delta_i = 2/\alpha_i$ is the path-loss dependent constant.

Proof: The probability of coverage can be evaluated as follows

$$\begin{aligned}\mathbb{P}_{cov} &= 1 - \Pr\left\{\max_{i=1\ldots K} P_i\zeta_i(\mathcal{S}_i) \le \tilde{\gamma}_{th}\right\}, \\ &= 1 - \prod_{i=1}^{K}\underbrace{\Pr\left\{\zeta_i < \frac{\tilde{\gamma}_{th}}{P_i}\right\}}_{\mathcal{F}_{\zeta_i}\left(\frac{\tilde{\gamma}_{th}}{P_i}\right)} \end{aligned} \tag{10}$$

where $\mathcal{F}_{\zeta_i}(x)$ is the CDF of the random variable $\zeta_i(\mathcal{S})$ derived in Proposition 1. ■

Remarks:

1) From (9), it follows that the downlink coverage probability is an increasing function of K, i.e., the number of tiers. Notice that the product term decreases with an increasing number of terms. Intuitively, the number of tiers and the density of RRHs determine the distributed diversity gain exercised by an MU by performing the best RRH selection. Increasing either will improve the coverage probability. However, increasing the number of tiers or RRH density will also increase the energy consumption.
2) It is easy to notice that the coverage probability is an increasing function of the cluster radius. This follows from the fact that increasing the cluster radius also increases the effective density of the RRHs which can be selected to serve the user. However like traditional diversity schemes the gains will become marginal after a certain value of $\mathcal{R}_c$. In fact, it can be shown that as $\mathcal{R}_c$ becomes large enough the coverage probability saturates and becomes independent of $\mathcal{R}_c$ (this follows from $\lim_{\mathcal{R}_c\to\infty}\gamma_l\left(\delta_i, \frac{\tilde{\gamma}_{th}\mathcal{R}_c^{\alpha_i}}{\tilde{P}_i}\right) \to \Gamma(\delta_i)$).

V. Upper-Bound on the Outage Capacity of K-Tier C-RAN

Employing the analytical machinery developed in the previous section, in this section our main objective is to characterize the bits/s/Hz performance of a K-tier C-RAN under a certain desired reliability constraint (ρ). To this end, the ρ-outage capacity of the C-RAN downlink is defined as

$$C_\rho = \sup\left\{C_o : \mathbb{P}_{out}(C_o) = \Pr\{\Gamma_{\boldsymbol{u}} \le 2^{C_o} - 1\} \le \rho\right\}. \tag{11}$$

In other words, C_ρ is maximum supportable rate for the downlink such that the outage probability for an MU remains below a pre-specified threshold ρ.

Proposition 3: The ρ-outage capacity of the MU in a K-tier C-RAN when all tiers suffer from small scale Rayleigh fading and large scale path-loss with the same path-loss exponent (α) can be upper-bounded as

$$C_\rho \le \log_2\left(1 + \frac{\left(\pi\Gamma(\delta+1)\sum_{i=1}^{K}\lambda_i\tilde{P}_i^{\delta}\right)^{\frac{1}{\delta}}}{\sigma^2\ln(\rho^{-1})^{\frac{1}{\delta}}}\right) \text{(bits/s/Hz)}. \tag{12}$$

Proof: From (9)

$$\mathbb{P}_{out}(C_o) = 1 - \mathbb{P}_{cov}|_{\gamma_{th}=2^{C_o}-1}. \tag{13}$$

To evaluate C_ρ, (9) needs to be inverted for C_o. In general, inverting (9) is complicated. However the closed form inversion is possible for an upper-bound when the path-loss exponent for all tiers is equal, i.e., $\alpha_i = \alpha$ as follows

$$\begin{aligned}\mathbb{P}_{cov} &\ge \lim_{r_o\to 0; R_c\to\infty} 1 - \prod_{i=1}^{K}\exp\Bigg[-\lambda_i\pi\Bigg\{r_o^2\exp\left(-\frac{\tilde{\gamma}_{th}r_o^{\alpha_i}}{\tilde{P}_i}\right) \\ &\quad + \delta_i\tilde{P}_i^{\delta_i}\tilde{\gamma}_{th}^{-\delta_i}\left(\gamma_l\left(\delta_i, \frac{\tilde{\gamma}_{th}\mathcal{R}_c^{\alpha_i}}{\tilde{P}_i}\right) - \gamma_l\left(\delta_i, \frac{\tilde{\gamma}_{th}r_o^{\alpha_i}}{\tilde{P}_i}\right)\right)\Bigg\}\Bigg], \\ &= 1 - \exp\left[-\sum_{i=1}^{K}\lambda_i\tilde{P}_i^{\delta}\pi\delta\tilde{\gamma}_{th}^{-\delta}\Gamma(\delta)\right]. \end{aligned} \tag{14}$$

From (13) the outage probability is given as

$$\mathbb{P}_{out}(C_o) \le \exp\left[-\sum_{i=1}^{K}\lambda_i\tilde{P}_i^{\delta}\pi\left((2^{C_o}-1)\sigma^2\right)^{-\delta}\Gamma(\delta+1)\right]. \tag{15}$$

Bounding (15) above by the reliability constraint ρ and inverting the equation for C_o concludes the proof. ■

Remarks:

1) From Proposition 3, it follows that C_ρ increases with an increase in the number of tiers. Effectively, increasing the number of tiers provides the power gain as expected due to distributed diversity.
2) Another interesting observation which follows from (12) is that the number of bits (reliability transmitted) in a unit time over one hertz of bandwidth can be improved by increasing either the transmit power of a tier or the density of RRHs in that tier.

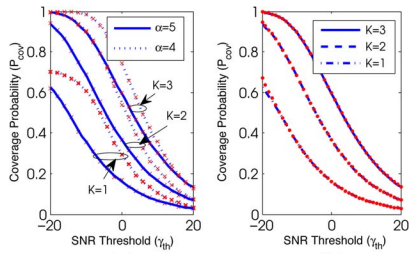

Fig. 1. Coverage probability for a K-tier C-RAN against varying desired SNR threshold with $\lambda_1 = 10^{-3}$, $\eta = 4$, $\sigma^2 = -20$ dBm, $P = 20$ dBm, $\beta = 10^{-1}$, $r_o = 0.1$ and $R_{cl} = 10$. (a) Solid and dashed lines correspond to the analytical results obtained from Eq. (9). Monte Carlo simulation results are indicated by red "×" markers. (b) Solid and dashed lines correspond to the analytical results obtained from Eq. (9) for $\alpha = 5$. Results obtained from the upper-bound in Eq. (1b) are indicated by red "•" markers.

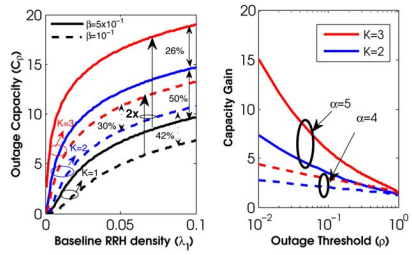

Fig. 2. Outage capacity and capacity gains for a K-tier C-RAN with with $\lambda_1 = 10^{-3}$, $\eta = 4$, $\sigma^2 = -20$ dBm, $P = 20$ dBm, $r_o = 0.1$ and $R_{cl} = 10$. (a) Outage capacity (b/s/Hz) for scheduled MU as a function of baseline density $\lambda_1$and number of tiers K for various values of β when $\alpha = 5$ and $\rho = 0.1$ are fixed. (b) Capacity Gains for K-tier C-RAN when compared to single tier architecture with varying permissible outage threshold ρ for $\beta = 5 \times 10^{-1}$.

VI. Results and Discussion

A. Validation of Analytical Results

Fig. 1(a) depicts the downlink coverage probability for an MU as a function of its desired SNR threshold for various values of K. Solid and dashed lines represent the analytical results obtained from (9) for fixed path-loss exponents, i.e., $\alpha = 5$ and 4 respectively. Monte Carlo simulation results are indicated by "×" markers and were performed by generating 10^4 realizations for both $\Pi = \cup_{k=1}^{K} \Pi_k$ and the fading-channel gains for each SNR threshold (γ_{th}). Without any loss of generality, the density of RRHs in the kth tier is expressed in terms of baseline density λ_1 as $\lambda_k = \eta^k \lambda_1$ where $\eta \geq 1$. In other words, each subsequent tier is assumed to be denser than its parent tier. Similarly, it is assumed that each tier employs decreasing transmit power which can be expressed in terms of baseline transmit power as $P_k = \beta^k P$ where $\beta \leq 1$.[1] As indicated by Fig. 1(a), analytical results are in good agreement with the Monte Carlo simulation results.

Fig. 1(b) compares the coverage probability from (9) against the upper-bound derived in (14) for varying SNR threshold, path-loss exponent and number of tiers. As illustrated by Fig. 1(b), the derived upper-bound is sufficiently tight and thus can be employed to further obtain tight bounds on outage capacity as in (12). It is obvious from Fig. 1 that the coverage probability decreases with an increase in the desired SNR threshold. Moreover, when the macro network is complemented by the deployment of cloud coordinated femto, pico, nano RRHs, the MU coverage probability can be significantly improved by employing the proposed user centric clustering mechanism.

B. Impact of Parametric Variations on Outage Capacity

Due to the space limitations, in this article, we only highlight the impact of important parametric variations on the downlink performance of a K-tier C-RAN. Fig. 2(a) plots the attainable outage capacity $(C_\rho$ bits/s/Hz) for a fixed desired threshold $\rho = 0.1$ against the varying baseline RRH density (λ_1). It is observed that with the dense tiered deployment where the transmit power of each subsequent tier is reduced by the factor of 10^{-1}, increasing K from 1 to 2 provides throughput gains which ranges between 40–50%. Moreover, the addition of a further tier with a similar power reduction for each RRH, further improves the downlink performance by 25–30%. It is observed that while the percentage gain in terms of bits/s/Hz is dependent upon the factor by which transmit power scales, i.e., β, the gain experienced in outage capacity $\mathcal{G} = C_\rho / C_\rho|_{K=1}$ is almost constant. Effectively, gains of about $\times 2$ are attainable with the proposed C-RAN association mechanism.

Fig. 2(b) shows that the outage capacity gain is indeed a function of desired reliability guarantee (expressed in terms of threshold ρ). The proposed user-centric RRH clustering algorithm provides gains which range from $\times 4$ to $\times 15$ depending upon the path-loss exponent and number of tiers when high reliability for operation of the link is desired (i.e., $\rho \to 0$). Intuitively the power gain extracted by exploiting distributed diversity (inherent in the RRH clustering mechanism) improves the received SNR significantly. In turn highly reliable links can be established to an MU with a significant capacity improvements realized by deploying additional tiers on top of macro-cells.

[1]Expressing transmit power and density in terms of the corresponding baseline parameters simplifies the exploration of the design space,but without obscuring insights due to a large number of design variables.

VII. Conclusion

In this letter, we have presented an analytical framework to characterize the coverage probability and the outage capacity of the heterogeneous cloud radio access network (C-RAN). We have investigated how distributed diversity can be exploited to realize throughput gains which are possible due to centralized signal processing in C-RANs. Lastly, we investigated the benefits of adding additional tiers and showed that capacity gains of about $\times 2$ can be realized by employing the proposed user centric remote radio head (RRH) clustering mechanism.

References

[1] "C-ran: The road towards green ran," Chn. Mobile Res. Instit., Beijing, China, 2011, White Paper, v. 2.5. [Online]. Available: http://labs.chinamobile.com/cran/wp-content/uploads/CRAN_white_paper_v2_5_EN.pdf

[2] K. Sundaresan, M. Y. Arslan, S. Singh, S. Rangarajan, and S. V. Krishnamurthy, "Fluidnet: A flexible cloud-based radio access network for small cells," in *Proc. 19th Annu. Int. Conf. Mobile Comput. Netw.*, 2013, pp. 99–110, ACM.

[3] T. Flanagan, "Creating cloud base stations with TI's keystone multicore architecture," Texas Instrum., Dallas, TX, USA, 2011, White Paper.

[4] C. Rowell, S. Han, Z. Xu, G. Li, and Z. Pan, "Towards green soft: A 5g perspective," *IEEE Wireless Commun. Mag.*, vol. 52, no. 2, pp. 66–73, Feb. 2014.

[5] Z. Ding and H. Poor, "The use of spatially random base stations in cloud radio access networks," *IEEE Signal Process. Lett.*, vol. 20, no. 11, pp. 1138–1141, Nov. 2013.

[6] C. Liu, K. Sundaresan, M. Jiang, S. Rangarajan, and G.-K. Chang, "The case for re-configurable backhaul in cloud-ran based small cell networks," in *Proc. IEEE INFOCOM*, 2013, pp. 1124–1132.

[7] A. Dawson, M. K. Marina, and F. J. Garcia, "On the benefits of ran virtualization in c-ran based mobile networks," in *Proc. EWSDN*, 2014, pp. 1–6.

[8] D. Stoyan, W. S. Kendall, J. Mecke, and L. Ruschendorf, *Stochastic Geometry and Its Applications*, vol. 2. Chichester, England: Wiley, 1995.